

# Wetting Controls Separation of Inertial Flows from Solid Surfaces

Cyril Duez,<sup>1</sup> Christophe Ybert,<sup>1</sup> Christophe Clanet,<sup>2</sup> and Lydéric Bocquet<sup>1,\*</sup>

<sup>1</sup>Laboratoire PMCN, Université Lyon 1, UMR CNRS 5586, 69622 Villeurbanne, France

<sup>2</sup>LadHyX, Ecole Polytechnique, UMR CNRS 7646, 91128 Palaiseau, France

(Received 17 October 2009; published 26 February 2010)

We investigate the flow of liquids around solid surfaces in the inertial regime, a situation commonly encountered with the so-called “teapot effect”, the annoying tendency for a liquid to trickle down the outside of a receptacle after pouring. We demonstrate that surface wettability is an unexpected key factor in controlling flow separation and trickling, the latter being completely suppressed in the limit of superhydrophobic substrates. This unforeseen coupling is rationalized in terms of an inertial-capillary adhesion framework, which couples inertial flows to surface wettability effects. This description of flow separation successfully captures the observed dependence on the various experimental parameters, wettability, flow velocity, solid surface edge curvature. As a further illustration of this coupling, a real-time control of flow separation is demonstrated using electrowetting for contact angle actuation.

DOI: 10.1103/PhysRevLett.104.084503

PACS numbers: 47.15.-x, 47.55.np, 68.08.-p

Over recent years, the development of superhydrophobic materials, exhibiting the so-called Lotus effect, has stirred up the physics of surfaces [1]. Their exceptional water repellency results from the combination of bare hydrophobicity and micro- or nano- structures decorating the solid surface. Because of their very high contact angle (and low hysteresis), liquids in contact with superhydrophobic surfaces exhibit remarkable dynamic properties, leading to intriguing phenomena like fast moving marbles [1], bouncing drops [2] or big splashes of impacting bodies [3]. Altogether these materials have opened the gate for new applications, the exploration of which is still in its infancy.

In this context we consider the potential role of superhydrophobic (SH) coatings—and more generally of wetting—on the separation of rapid flows around solid surfaces. In every day life, this phenomenon is called the “teapot effect” [4–8]: a “rapid” water flow poured from a teapot is shown to bend and finally flow around the spout as the velocity decreases; see Fig. 1(a) and [9]. This phenomenon is usually interpreted in terms of the bending of stream lines and flow separation [4–6,10], while viscosity and surface wettability are not taken into account. This is *a priori* in agreement with the relatively high Reynolds and Weber numbers,  $Re$ ,  $We$ , characterizing these rapid—inertial—flows (with  $Re = \rho Ua/\eta$ ,  $We = \rho U^2a/\gamma$ , with  $\gamma$  a typical surface energy,  $\eta$  the shear viscosity,  $a$  a typical length scale,  $U$  a velocity,  $\rho$  the mass density). In the opposite regime of low Reynolds and Weber numbers, capillary and viscous effects are expected, as, e.g., observed in the work by Kistler and Scriven using highly viscous fluids [7].

We show in this Letter that in contrast to the expectations in the inertial regime, wettability is an unforeseen key parameter in the flow separation of liquids around solid bodies. As a paradigm, the teapot effect is fully eliminated by making the spout superhydrophobic; see Fig. 1 and [9].

More fundamentally, this result points to an *a priori* unexpected link between water repellency and large scale flows. It provides a novel example of an inertial-capillary effect coupling wetting to inertial fluid dynamics, as also observed in previous works [11].

To get further insight into the physical mechanisms at the origin of this phenomenon, we have performed a systematic study of the ejection and flow separation of liquids in a controlled geometry, with varying surface properties and geometrical characteristics. The setup is sketched in Fig. 2: a water jet with velocity  $U$ —typically from 1 to  $5 \text{ m} \cdot \text{s}^{-1}$  in our study—, and diameter  $D$ —here  $D = 4 \text{ mm}$ —impacts and spreads over the “impacter.” The latter consists in horizontal disks of diameter  $D_{\text{imp}} = 15 \text{ mm}$ , ended by a curved edge characterized by its radius of curvature  $r_i$  ( $r_i = 2, 1, 0.5, 0.03 \text{ mm}$ ). The wettability of the impacters is tuned by using different chemical processes, leading to a static (advancing) contact angle  $\theta_0$  ranging between  $10^\circ$  up to  $175^\circ$  (superhydrophobic coating). A contact angle of  $\theta_0 = 78 \pm 5^\circ$  is obtained for

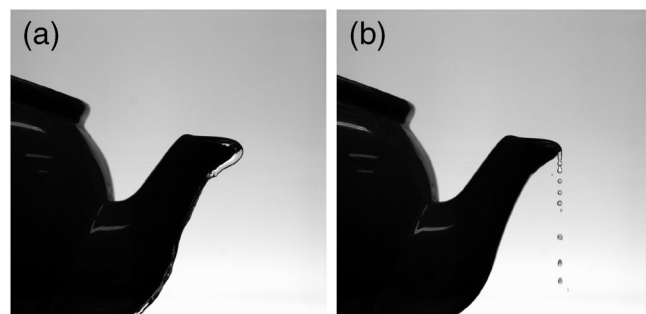


FIG. 1. (a) Water flow under the spout of a hydrophilic teapot, exhibiting bending and flow around the spout as the water velocity decreases. (b) In contrast, a teapot with a superhydrophobic spout (here black soot) avoids this effect for any velocity.

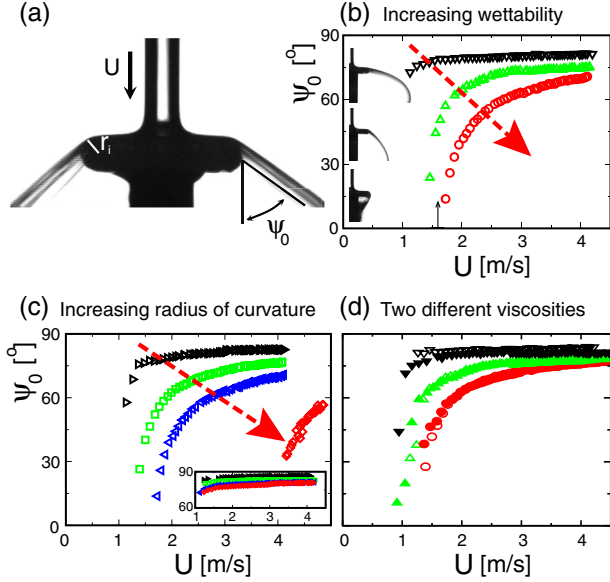


FIG. 2 (color online). Flow ejection versus wettability, geometry, and viscosity. (a) Geometry of the impacting flow. (b)  $\psi_0(U)$  for various impacters with increasing wettability (same  $r_i = 1$  mm): from top to bottom,  $\theta_0 = 175^\circ$ ,  $115^\circ$ ,  $10^\circ$ . Inset: images of the deflections at a given velocity  $U = 1.65 \pm 0.05$  m  $\cdot$  s $^{-1}$  (arrow on the  $U$  axis). (c)  $\psi_0(U)$  for various impacters with increasing  $r_i$  (same  $\theta_0 = 10^\circ$ ): from top to bottom  $r_i \approx 0.03$ ,  $0.5$ ,  $1$ ,  $2$  mm. Inset: same with  $\theta_0 = 175^\circ$  (same symbols). (d)  $\psi_0(U)$  for liquids with two different viscosities: water  $\eta_w = 1$  mPa  $\cdot$  s (closed symbols); and a water-glycerol mixture, with twice the viscosity  $\eta_{w/g} = 2$  mPa  $\cdot$  s (open symbols). From top to bottom,  $\theta_0 = 175^\circ$ ,  $115^\circ$ ,  $10^\circ$ , and  $r_i = 0.5$  mm. Ejection angles  $\psi_0(U)$  are found to coincide for the two liquids.

cleaned, native purum aluminum (Al 1050) impacters. A treatment in a UV- $O_3$  reactor lead to a strongly hydrophilic impacter with a contact angle decreasing to  $\theta_0 = 10 \pm 5^\circ$ . Hydrophobic impacters were obtained by grafting fluoro-silane chains (perfluoro-octyltriethoxysilane) on the aluminum surface, leading to  $\theta_0 = 115 \pm 5^\circ$ . Finally, superhydrophobic impacters were obtained using galvanic deposition on purum copper (Cu-OF) impacters [12].

For these different impacters, we measured the ejection angle  $\psi_0$  (defined in Fig. 2) versus fluid velocity  $U$ , for various wettabilities ( $\theta_0$ ), geometries ( $r_i$ ) and fluid viscosities. The angle  $\psi_0$  is measured from the detailed image analysis of the fluid surface. Our results are gathered in Figs. 2(b)–2(d). Altogether, these experiments demonstrate that the wettability of the surface has a key influence on the ejection of the fluid film from the surface, Fig. 2(b). Furthermore superhydrophobic impacters, characterized by a static contact angle close to  $180^\circ$ , strongly eject the liquid film, thereby avoiding trickling along the solid surface. Also, as one intuitively expects, the radius of curvature of the impacter is found to have a strong influence on ejection, Fig. 2(c). But again, superhydrophobicity is found to prevail over this geometrical parameter, as demonstrated

in the inset of Fig. 2(c), where only a weak dependence of the ejection angle on velocity is measured for superhydrophobic impacters.

Viscosity is found *not* to be a relevant parameter for the present “fast flow” experiment, as one expects in the inertial regime: as shown in Fig. 2(d), the ejection does not depend on the viscosity of the fluid. This observation implicitly dismisses a viscocapillary origin of the phenomenon. This is consistent with the rather large Reynolds number characterizing the flow,  $Re_\ell = U\ell/\nu$ :  $Re_D \sim 10^4$  for  $\ell = D$ , the initial jet diameter, while  $Re_e \sim 500 - 10^3$  with  $\ell = e_0$ , the film thickness  $e_0$ . Here the film thickness  $e_0$  is estimated using mass flux conservation as  $e_0 \approx D^2/4D_{\text{imp}}$  with  $D$  the liquid jet diameter and  $D_{\text{imp}}$  that of the impacter [13]. Note also that gravity effects, as quantified by a Froude number  $Fr = g\ell/U^2$  with  $g$  the gravity constant, play a negligible role here.

Finally, a threshold for trickling along the impacter can be identified experimentally: below a minimum velocity  $U_c$ , the liquid is not ejected from the impacter anymore but flows along the spout; see insets in Fig. 2(b). We gather in Fig. 3(a) the results for the threshold velocity—here plotted in terms of a dimensionless Weber number—as a function of the wettability of the impacter and its radius of curvature. As intuitively expected, trickling along the surface occurs more easily for spouts with thicker edges. On the other hand, superhydrophobic coatings lead to flow separation whatever the radius of curvature of the edge. Furthermore, these plots suggest a linear dependence of the threshold Weber number,  $We_c$ , versus  $1 + \cos\theta_0$ , with a prefactor depending strongly on the impacter’s radius of curvature  $r_i$ , Fig. 3(b).

Altogether these experimental observations points to the three key parameters controlling flow separation: the inertia of the fluid, the curvature of the “spout” and more unexpectedly its wettability. Trickling along the solid surface is fully avoided in the limit of sharp edges or superhydrophobic surfaces. However the underlying physical

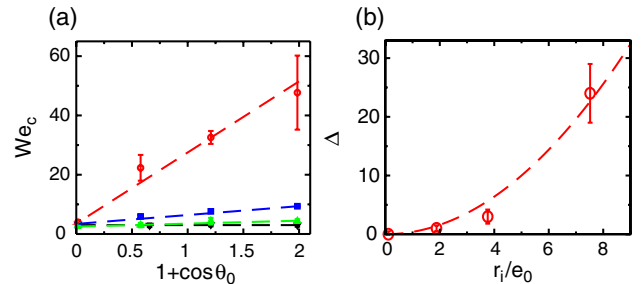


FIG. 3 (color online). (a) Threshold Weber number for trickling along the impacter,  $We_c = \rho U_c^2 e_0 / \gamma$ , versus wettability  $1 + \cos\theta_0$ , for various radius of curvature of the impacter’s edge: from bottom to top  $r_i \approx 0.03$ ,  $0.5$ ,  $1$ , and  $2$  mm. Dashed lines are linear fits with slope  $\Delta$ . (b) Plot of the slope  $\Delta$  versus radius of curvature  $r_i$ . The dashed line is a fit according to the expected scaling for the slope as  $(r_i/e_0)^2$ , in Eq. (2).

mechanism remains to be discovered: how to couple fast (inertia dominated) flows with wettability effects?

We rationalize these observations in terms of an “inertial-capillary” mechanism. The key point underlying the proposed mechanism is the existence of a capillary meniscus connecting the flow to the spout’s surface. This is illustrated in Fig. 4, showing the experimental picture of a cut of the liquid interface under flow, obtained using a laser sheet and a fluorescent dye: one does indeed expect that the liquid interface should connect the solid surface with an imposed angle given by the wetting contact angle  $\theta_0$ .

Now, to be predictive on the ejection, one should solve the inertial fluid dynamics (Euler equation) inside the liquid sheet with free surfaces [10], completed by the condition of a finite contact angle at the flow separation, fixed by wetting thermodynamics. This is a challenging task, which, to our knowledge, has not been solved in the literature. Therefore, in order to capture semiquantitatively the above mechanism, we merely consider the momentum balance for the liquid sheet. As sketched in Fig. 4, the deflection of the sheet is associated with a variation of momentum flux: this flux variation should thus be compensated by an “adhesive” contribution pointing towards the solid. Following this line, we now estimate both components of this momentum balance.

We consider the regime of large fluid velocity  $U$ , where the deviation  $\delta\psi_0 = \frac{\pi}{2} - \psi_0$  of the water sheet is small. This deflection leads to a variation of momentum flux, here denoted as  $\mathcal{D}(U)$  and defined as the mass flux times the velocity:  $\mathcal{D}(U) = \rho_w U^2 e_0 (1 - \sin\psi_0) \approx \frac{1}{2} \rho_w U^2 e_0 \delta\psi_0^2$  (per unit axisymmetric length and projected on the horizontal direction  $x$ ).

Now the adhesive component of the momentum balance takes its origin in the (negative) pressure drop in the liquid,  $\Delta P$ , induced by the bending of the streamlines, and clas-

sically quoted as Coanda effect [14]. As depicted in Fig. 4, the pressure drop acts over a “wetted area”,  $\mathcal{A}_{\text{wet}} \approx r_i \delta\psi_{\text{wet}}$  (per unit axisymmetric length), providing an estimate for the “adhesive” force as  $F_{\text{adh}} \sim \Delta P \times \mathcal{A}_{\text{wet}}$ . Projected along the horizontal, this yields  $F_{\text{adh}}^x \approx \mathcal{A}_{\text{wet}} \times \Delta P \times \frac{\delta\psi_{\text{wet}}}{2}$ . The pressure drop  $\Delta P$  due to the bending of the streamlines is classically estimated using Bernoulli theorem: denoting  $\mathcal{R}$  the radius of curvature of the flow streamlines, then one expects  $\Delta P \approx -\rho_w U^2 e_0 / \mathcal{R}$  [14]. Typically,  $\mathcal{R}$  may be estimated as an averaged radius over the fluid film thickness  $e_0$ , which we write  $\mathcal{R} = r_i + \alpha e_0$ , with  $\alpha \approx \frac{1}{2}$ . Now, a key point is to connect the wetted area  $\mathcal{A}_{\text{wet}}$ —and thus the adhesion force—to the location and geometry of the capillary meniscus, as characterized by its contact angle  $\theta_0$  and edge radius of curvature  $r_i$ . This is a classical problem in capillarity [15,16], with, e.g., applications in adhesive granular materials [17]. We follow this standard line of description here. First, the curvature of the meniscus,  $\mathcal{C}$ , is fixed by the pressure drop  $\Delta P$ , as  $\mathcal{C} = |\Delta P| / \gamma$  ( $\gamma$  the liquid vapor surface tension). Then, using a circle approximation for the meniscus, see, e.g., [16], one obtains the extension  $\delta\psi_{\text{menisc}}$  of the meniscus as  $\delta\psi_{\text{menisc}}^2 = 2\mathcal{C}^{-1} / r_i \times (1 + \cos\theta_0)$ . This leads to the final expression for the wetted area  $\mathcal{A}_{\text{wet}} = r_i \delta\psi_{\text{wet}}$  with  $\delta\psi_{\text{wet}} = \delta\psi_0 + \delta\psi_{\text{menisc}}$ , and  $\delta\psi_{\text{menisc}} = [2\gamma(1 + \cos\theta_0) / r_i |\Delta P|]^{1/2}$ .

Gathering these different results, one may write the momentum balance as:  $\frac{1}{2} \rho_w U^2 e_0 \delta\psi_0^2 \approx \frac{1}{2} |\Delta P| r_i (\delta\psi_0 + \delta\psi_{\text{menisc}})^2$ . Using the previous results, this leads to the following expression for the flow deviation:

$$\delta\psi_0 = \sqrt{\mathcal{F} \left[ \frac{r_i}{\mathcal{R}} \right] \frac{(1 + \cos\theta_0)}{\text{We}}}, \quad (1)$$

where  $\text{We} = \rho U^2 e_0 / \gamma$  is the Weber number constructed on the film thickness  $e_0$ , and the geometrical factor  $\mathcal{F}[r_i/\mathcal{R}] \approx 2(1 - \sqrt{r_i/\mathcal{R}})^{-2}$  scales as  $\mathcal{F} \sim (r_i/e_0)^2$  for  $r_i/e_0 \gg 1$ .

A few comments are in order. First, as announced, this inertial-capillary description does indeed connect the large scale fluid properties to the surface properties: *via* its geometry but more interestingly *via* its surface properties and contact angle  $\theta_0$ . Furthermore, it fully reproduces all experimental observations in Fig. 2: the angle of deviation  $\psi_0 = \pi/2 - \delta\psi_0$  is indeed predicted to increase with the fluid velocity ( $U$ , or  $\text{We}$ ), as well as with the contact angle of the surface ( $\theta_0$ ); also  $\psi_0$  decreases with the radius of curvature of the spout ( $r_i$ ).

It is finally interesting to address the trickling transition and the corresponding threshold velocity, plotted in Fig. 3. The above simplified argument does not predict intrinsically a limit of stability for the flow. However, as suggested by the experiments, one may assume that flow separation does not occur anymore below a threshold (minimum) flow deviation  $\delta\psi_0 = \delta\psi_0^{\text{min}}$ . Equation (1) then suggests a

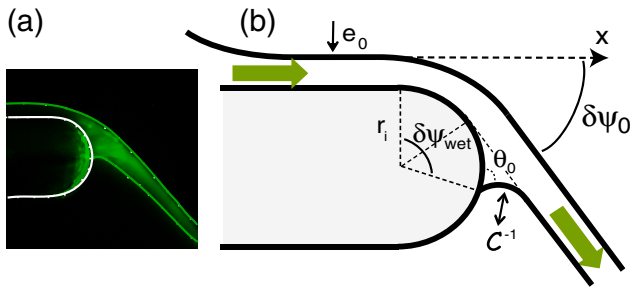


FIG. 4 (color online). (a) Experimental picture of a cut of the liquid interface under flow. Solid lines are a guide for the eye of the various interfaces. (b) Details of the flow around the edge of the impactor. The fluid film with thickness  $e_0$  bends around the edge of the impactor, with radius of curvature  $r_i$ ;  $\delta\psi_0 = \frac{\pi}{2} - \psi_0$  is the deflection angle and  $\delta\psi_{\text{wet}}$  the angular range of the curved wetted area ( $\delta\psi_{\text{wet}} = \delta\psi_0 + \delta\psi_{\text{menisc}}$  with  $\delta\psi_{\text{menisc}}$  the angular width of the meniscus).



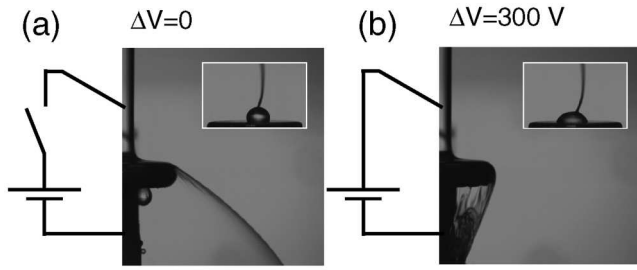


FIG. 5. Electrowetting control of flow separation: A tunable wettability of the surface is achieved by imposing various electric potential drop  $\Delta V$  between the liquid and the solid surface (insets). This leads to an active control of the ejection and flow of the liquid along the impactor: flow ejection is obtained for  $\Delta V = 0$ , while trickling is induced for  $\Delta V = 300$  V.

corresponding threshold Weber scaling as

$$\text{We}_c \propto \frac{r_i^2}{e_0^2} (1 + \cos\theta_0). \quad (2)$$

This prediction is compared to the experimental results in Fig. 3, showing again a very good agreement: both the predicted linear scaling on  $1 + \cos\theta_0$  [Fig. 3(a)] and the dependence of its slope on  $r_i$  [Fig. 3(b)] reproduce the experimental results. Altogether, the inertial-capillary picture is seen to capture the main features of the teapot effect. It solves accordingly the flow separation question in terms of a novel, capillary meniscus, ingredient. We finally note that this inertial-capillary picture differs strongly from the viscosity-dependent splash mechanism in [3]: in contrast to splashes, the capillary meniscus is here stationary and wetting *dynamics* is thus not relevant for the flow separation mechanism.

Beyond this understanding, our results suggest that the flow pattern may be directly controlled *via* a tuning of surface wetting properties. As shown in recent years, electrowetting is a very efficient solution to tune the surface properties and the application of an electric potential drop on a polarized surface leads to a direct modification of the contact angle [18]. We have coupled our geometry in Fig. 2 to an electrowetting setup, Fig. 5 [9]. An electric drop  $\Delta V$  applied between the liquid and the impactor allows tuning of the contact angle on the impactor between  $\theta_0 = 110^\circ$  to  $\theta_0 = 60^\circ$  as  $\Delta V$  is varied between 0 and 300 V; see insets of Fig. 5. Now, when a liquid jet impacts the liquid surface, we observe that the ejection of the fluid can be tuned directly—and dynamically—by the applied potential drop  $\Delta V$ . This is illustrated in Fig. 5, where trickling along the surface is induced under an applied potential drop

[Fig. 5(b)], while the fluid is ejected when this applied potential drop is absent. Such an active control opens new application perspectives to dynamically shape flow patterns [19].

To summarize, we have demonstrated the crucial influence of surface wettability on separation of rapid flows. As a paradigm superhydrophobic surfaces fully avoid trickling, and thus beat the teapot effect. Experimental results are rationalized on the basis of an inertial-capillary adhesion phenomenon, coupling inertial flows to a capillary adhesion mechanism. This phenomenon effectively bridges the gap between the small (surface) and large (flow) scales.

This project was supported by DGA. We thank Jacques Tardy (INL) for the parylene coatings.

\*lyderic.bocquet@univ-lyon1.fr

- [1] D. Quéré, Rep. Prog. Phys. **68**, 2495 (2005).
- [2] D. Richard, C. Clanet, and D. Quéré, Nature (London) **417**, 811 (2002).
- [3] C. Duez, C. Ybert, C. Clanet, and L. Bocquet, Nature Phys. **3**, 180 (2007).
- [4] J. Walker, Sci. Am., **251**, No. 4, 144 (1984).
- [5] M. Reiner, Phys. Today, **9**, No. 9, 16 (1956).
- [6] J. B. Keller, J. Appl. Phys. **28**, 859 (1957).
- [7] S. F. Kistler and L. E. Scriven, J. Fluid Mech. **263**, 19 (1994).
- [8] H. Isshiki, B. S. Yoon, and D. J. Yum, Phys. Fluids **21**, 082104 (2009).
- [9] See supplementary material at <http://link.aps.org/supplemental/10.1103/PhysRevLett.104.084503> for movies and electrowetting details.
- [10] J.-M. Vanden-Broeck and J. B. Keller, Phys. Fluids **29**, 3958 (1986).
- [11] J. C. Bird, S. Mandre, and H. A. Stone, Phys. Rev. Lett. **100**, 234501 (2008).
- [12] I. A. Larmour, S. E. J. Bell, and G. C. Saunders, Angew. Chem., Int. Ed. **46**, 1710 (2007).
- [13] C. Clanet, Annu. Rev. Fluid Mech. **39**, 469 (2007).
- [14] E. Guyon, J.-P. Hulin, and L. Petit, *Physical Hydrodynamics* (Oxford University Press, Oxford, 2001).
- [15] J. Israelachvili, *Intermolecular and Surface Forces* (Academic Press, London, 1992), Chap. 15.6, 2nd ed.
- [16] F. L. Orr, L. E. Scriven, and A. P. Rivas, J. Fluid Mech. **67**, 723 (1975).
- [17] L. Bocquet, E. Charlaix, S. Ciliberto, and J. Crassous, Nature (London) **396**, 735 (1998).
- [18] F. Mugele and J. C. Baret, J. Phys. Condens. Matter **17**, R705 (2005).
- [19] C. Duez, C. Ybert, C. Clanet, and L. Bocquet, patents pending, PCT/EP2009/064474 and FR0857782.